ACS APPLIED MATERIALS & INTERFACES

Research Article

www.acsami.org

Optimization of Surface Coating on Small Pd Nanosheets for in Vivo near-Infrared Photothermal Therapy of Tumor

Saige Shi,[†,‡] Yizhuan Huang,[†] Xiaolan Chen,[*,†] Jian Weng,[‡] and Nanfeng Zheng[*,†]

[†]State Key Laboratory for Physical Chemistry of Solid Surfaces, Collaborative Innovation Center of Chemistry for Energy Materials and Department of Chemistry, College of Chemistry and Chemical Engineering, Xiamen University, Xiamen 361005, P.R. China

[‡]Research Center of Biomedical Engineering, Department of Biomaterials, College of Materials, Xiamen University, Xiamen 361005, P.R. China

Supporting Information

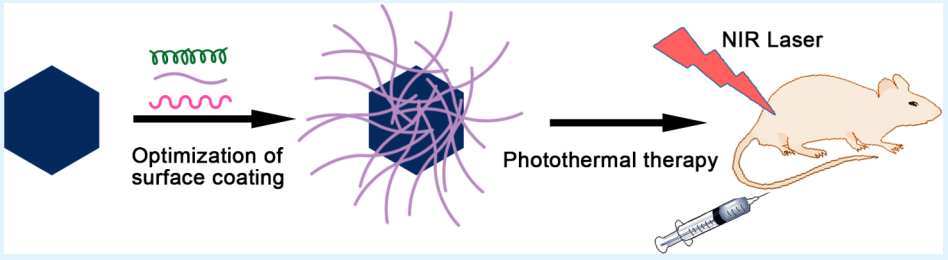

ABSTRACT: Palladium nanosheets with strong near-infrared absorption have been recently demonstrated as promising photothermal agents for photothermal therapy (PTT) of cancers. However, systematic assessments of their potential risks and impacts to biological systems have not been fully explored yet. In this work, we carefully investigate how surface coatings affect the in vivo behaviors of small Pd nanosheets (Pd NSs). Several biocompatible molecules such as carboxymethyl chitosan (CMC), PEG-NH_2, PEG-SH, and dihydrolipoic acid-zwitterion (DHLA-ZW) were used to coat Pd NSs. The blood circulation half-lives, biodistribution, potential toxicity, clearance, and photothermal effect of different surface-coated Pd NSs in mice after intravenous injection were compared. PEG-SH-coated Pd NSs (Pd-HS-PEG) were found to have ultralong blood circulation half-life and show high uptake in the tumor. We then carry out the in vivo photothermal therapeutic studies on the Pd-HS-PEG conjugate and revealed its outstanding efficacy in in vivo photothermal therapy of cancers. Our results highlight the importance of surface coatings to the in vivo behaviors of nanomaterials and can provide guidelines to the future design of Pd NSs bioconjugates for other in vivo applications.

KEYWORDS: *palladium, nanosheet, surface coating, in vivo behaviors, photothermal therapy*

1. INTRODUCTION

The rapid development of nanotechnology has been increasing the likelihood of engineered nanoparticles coming into contact with humans as drug carriers or contrast agents.[1−3] However, before novel functional nanoparticles are readily translated into the clinical settings, the blood circulation, biodistribution, clearance as well as potential toxicity need to be well-investigated.[4−7] It has been recognized that many properties of nanomaterials, such as particle size, shape, composition, surface charge, surface chemical functionality, and so on, affect their in vivo behaviors.[8,9] Among these properties, surface ligand modification plays an important role in improving aqueous solubility and stability of various nanomaterials in physiological environments,[10−12] and prolonging circulation time in blood and reducing the nonspecific accumulation in some reticuloendothelial system (RES) organs such as liver and spleen.[13−15]

Polymers based on polyethylene glycol (PEG) have widely used for the surface modification of various bionanomaterials, particularly those for in vivo applications. PEG is a relatively inert hydrophilic polymer that has been shown to alleviate nanotoxicity and permit the particles to escape RES.[16] The incorporation of PEG onto the surfaces of nanoparticles can significantly improve the circulation time in vivo.[17] Besides PEG, polysaccharides and zwitterionic ligands have gained increasing attention as well. For example, heparin and dextran coated poly(methyl methacrylate) nanoparticles has been demonstrated to dramatically increase their in vivo circulation time compared to unmodified particles.[18] As blood pool contrast agents, magnetite nanoparticles modified by zwitterionic ligands displayed prolonged in vivo circulation time.[19]

Because of their strong and well-defined near-infrared (NIR) surface plasma resonance (SPR) properties as well as significantly high photothermal stability and excellent biological compatibility, two-dimensional (2D) Pd nanosheets are a new type of promising photothermal agents for application in cancer photothermal therapy (PTT).[20−24] Recently, ultrasmall 2D Pd nanosheets (Pd NSs) with an average diameter of 4.4 nm have

Received: April 10, 2015
Accepted: June 15, 2015
Published: June 15, 2015

DOI: 10.1021/acsami.5b03106
ACS Appl. Mater. Interfaces 2015, 7, 14369−14375

been successfully prepared.[23] With the surface modification by glutathione (GSH), the ultrasmall Pd NSs exhibit prolonged blood circulation and higher tumor accumulation, and can even be efficiently cleared from the body through urine.[23] Encouraged by these results, in the current work, we further explore other surface ligands, such as PEG-NH_2, carboxymethyl chitosan (CMC), PEG-SH, and DHLA-ZW (Scheme 1), on the

Scheme 1. Surface Modification of Pd Nanosheets (Pd NSs) with Different Ligands

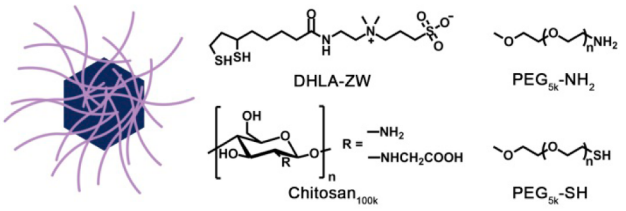

influence of circulation time, biodistribution, potential toxicity, clearance and photothermal therapy of these ultrasmall 2D Pd nanosheets in vivo and hope to obtain the best optimum surface modification for their biomedical applications.

2. MATERIALS AND METHODS

2.1. Materials. All chemicals were obtained from commercial suppliers and used without further purification. Palladium(II) acetylacetonate ($Pd(acac)_2$), N,N-dimethylpropionamide (DMP) and poly(vinylpyrrolidone) (PVP, MW = 30 kDa) were purchased from Sigma-Aldrich. Methoxypoly(ethylene glycol)thiol (PEG-SH, MW = 5 kDa) and methoxypoly(ethylene glycol)amine (PEG-NH_2, MW = 5 kDa) were obtained from Xiamen Sinopeg Biotech, Inc.. Carboxymethyl chitosan (MW = 100 kDa) were purchased from Zhejiang Aoxing biotech, Inc.

2.2. Characterization. Transmission electron microscopy (TEM) images were obtained using a TECNAI F-30 high resolution transmission electron microscope operating at 300 kV. UV−vis-NIR absorption spectra were measured with a Cary 5000 UV/vis/NIR spectrophotometer (Varian). Fourier transform infrared (FTIR) spectra were performed on a JASCO FT/IR-460 PLUS spectrometer (Tokyo) at room temperature. The Pd contents in tissue and fluid samples were analyzed by an inductively coupled plasma mass spectrometry (ICP-MS, Agilent 7700).

2.3. Synthesis of Ultrasmall Pd Nanosheets (Pd NSs). Ultrasmall Pd NSs were synthesized according to our previously published procedures.[23] Briefly, 10 mg of $Pd(acac)_2$, 30 mg of PVP, and 30.6 mg of NaBr were dissolved in a mixed solvent of DMP (2 mL) and water (4 mL). The resulting yellow solution was left undisturbed at room temperature overnight and then transferred to a glass pressure vessel. After being charged with CO to 1 bar, the vessel was heated at 100 °C and kept at this temperature for 2 h with stirring before being cooled to room temperature.

2.4. Surface Modification of Pd NSs with Different Ligands. Modification of the as-made Pd NSs with PEG-NH_2, CMC, PEG-SH, or DHLA-ZW was performed as following: First the Pd NSs was purified by the mixture solution of ethanol (1 mL) and acetone (8 mL) once to remove excessive surfactants and ions. Then they were diluted by solution containing different ligands and shaken for 2 h. After ultrafiltration with PBS to remove unbound ligands, the various modified Pd NSs solution was stored at 4 °C for future use.

2.5. Cell Culture. HeLa cell line was purchased from the cell storeroom of Chinese Academy of Science and cultured in RPMI-1640 medium containing 10% calf serum and 1% penicillin/streptomycin at 37 °C under 5% CO_2. For the cell toxicity assay, HeLa cells were precultured in two 96-well plates at the density of ~1×10^4 per well for 12 h and then added with various modified Pd NSs at different concentrations. After incubation for another 24 h, cell viabilities were measured by the standard MTT (3-(4,5)-dimethylthiahiazo-2-yl)-2,5-diphenyltetrazolium bromide) assay.

2.6. Animals and Tumor Implantation. All animal experiments were performed according to the guidelines of Animal Management Rules of the Ministry of Health of the People's Republic of China and the guidelines for the Care and Use of Laboratory Animals of China. Female Kunming mice (~20 g, 6−8 weeks old) used in this study were provided by the Laboratory Animal Center of Xiamen University. The S180 tumor model was implanted by subcutaneous injecting S180 cells into the right rear legs in the mice.

2.7. In Vivo Pharmacokinetics, Biodistribution, and Renal Clearance Kinetic Studies of Surface-Coated Pd NSs. For pharmacokinetic studies, the S180 tumor-bearing mice were intravenously injected with different modified Pd NSs (10 mg/kg) and the blood samples were collected from orbital at 10 min, 20 min, 0.5, 1, 2, 4, 8, 12, 24, and 36 h, respectively. These blood samples were lysed with HNO_3 and H_2O_2 mixture solution and the Pd concentrations were measured by ICP-MS.

To evaluate the tissue distributions of various functionalized Pd NSs, the S180 tumor-bearing mice were intravenously injected with different Pd NSs (1 mg/mL, 200 μL) and sacrificed at 1 h, 8 h, 24 h, 7 days, and 28 days post injection (n = 4 for each time point). The organs and tumors were collected, weighted and partly lysed by HNO_3 and H_2O_2 mixture solution. The Pd concentrations (percentage of injected dose per gram of organ, %ID/g) were measured by ICP-MS.

In renal clearance kinetic studies of Pd NSs, urine was collected in metabolism cage with special precaution to avoid fecal contamination. After intravenous injection of 200 μL Pd-HS-PEG (1 mg/mL, n = 3), the mice without tumors were closed in the metabolism cages to collect the urine for 3 days. The urine samples were lysed with HNO_3 and H_2O_2 mixture solution. The Pd concentrations in the urine samples were measured by ICP-MS method.

2.8. Hematology and Histology Studies. After the intravenous injection of 200 μL (1 mg/mL, n = 5 for each group) Pd NSs for 7 days, an approximate 0.3 mL of blood from each mouse was collected from eye socket for the blood chemistry test containing AST and ALT using microplate reader Infinite M200.

For histology examinations, major organs including liver, kidney, spleen, heart, and lung from mice were collected after injecting surface-modified Pd NSs for 28 days, fixed with 8% neutral buffered formalin, processed routinely into paraffin, sectioned at 5 μm, stained with hematoxylin and eosin (H&E) and examined by a digital microscope. Statistics were based on standard deviations of 3 mice per group.

2.9. In Vivo NIR Imaging and Therapeutic Efficacy. After the intravenous injection of 300 μL (1 mg/mL, n = 5 for each group) Pd-HS-PEG or PBS for 24 h, the S180 tumor-bearing mice were exposed to the 808 nm laser with a power density of 0.4 W/cm^2 for 5 min, an infrared thermography (HM-300, Guangzhou SAT Infrared Technology Co., Ltd.) was used to capture the temperature change on the site of the tumor. After the treatment, the tumor volume was calculated every 2 days as length × $(\text{width})^2$ × 1/2 with a caliper. The relative tumor volume was calculated as V/V_0, V_0, and V stand for the tumor volume on the first day and on the day of measurement, respectively.

3. RESULTS AND DISCUSSION

3.1. Surface-Coated Small Pd Nanosheets by PEG-NH_2, CMC, PEG-SH, and DHLA-ZW. Several ligand molecules, including PEG-NH_2, carboxymethyl chitosan (CMC), PEG-SH and dihydrolipoic acid zwitterionic ligand (DHLA-ZW), were used to coat small Pd nanosheets (Pd NSs) (Scheme 1). By dispersing Pd NSs in these ligand solutions and reacting for 2 h, finally removing of excess ligands by ultrafiltration, we obtain excellent suspensions of Pd NSs stabilized in PBS by these surface modifiers (Figure S1, Supporting Information). Because of the presence of PVP, the original synthesized Pd NSs were highly negatively charged. After coating different ligands to the Pd NSs, the zeta potentials of Pd−H_2N-PEG, Pd-CMC, Pd-HS-PEG and Pd-DHLA-ZW

DOI: 10.1021/acsami.5b03106
ACS Appl. Mater. Interfaces 2015, 7, 14369−14375

are about −5, +22.6, −5, and −9 mV (Table S1, Supporting Information), respectively. As shown in Figure 1a, the

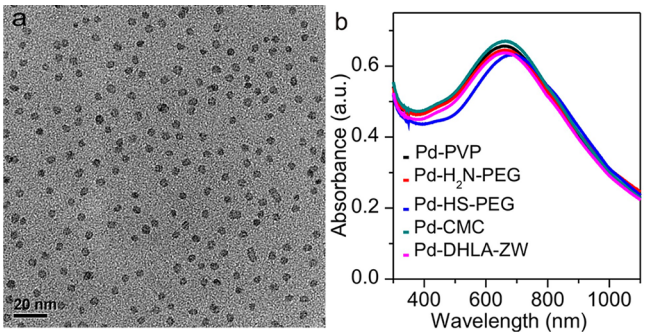

Figure 1. (a) Typical TEM images of Pd-HS-PEG. The pictures for other surface-modified Pd NSs are similar to the Pd-HS-PEG with not shown. (b) UV−vis−NIR absorption spectra of different surface-coated Pd NSs.

transmission electron microscopy (TEM) images indicated that the as-prepared surface-modified Pd NSs are monodisperse with diameter of ∼4.4 nm. In addition, these surface-coated Pd NSs still display well-defined and strong SPR absorption in the NIR region just like native synthesized Pd NSs with PVP modification (Figure 1b).

3.2. In Vivo Blood Circulation, Biodistribution Studies of Surface-Coated Pd NSs. The blood concentration and circulation time as well as biodistribution of drugs in vivo are highly correlated with their efficacy in most cases. As for nanoparticle systems, their cancer therapy efficacy is often compromised by the fact that most nanoparticles are rapidly cleared from the blood by the immune system. The surface adsorption of plasma proteins (opsonins) on nanoparticles results in their easy recognition by macrophages in liver and spleen, followed by phagocytosis and elimination.[25] To prolong the circulation time, it is thus critical to give nanoparticles more contact time to accumulate at the target tissues. Surface modification with different molecules to form a "corona" outside the nanoparticle is often used to suppress the interaction of nanoparticles with proteins and delay the reticuloendothelial system (RES) uptake. Poly(ethylene glycol) (PEG) is the most commonly applied nonionic hydrophilic polymer to impart nanoparticles with functionality, water solubility, biocompatibility and stealth for reducing nonspecific accumulation and prolonging the blood circulation so that nanoparticles can effectively target tumors through the well-known enhanced permeability and retention (EPR) effect.[26,27] In this study, we first investigated the effect of PEG-NH_2 (5 kDa), which interacts with Pd NSs by amine groups. To evaluate the blood concentration, circulation time and tissue distributions of the PEG-NH_2-functionalized Pd NSs (Pd−H_2N-PEG), the S180 tumor-bearing mice were intravenously injected with Pd−H_2N-PEG, the blood samples were collected from eye socket at different time points and the mice were sacrificed at 1 h, 8 h, 24 h, 7 days, and 28 days post injection (n = 4 for each time point). Four main tissues/organs including liver, spleen, kidney and tumor were collected and digested. The Pd amounts in these tissues and blood samples were measured by ICP-MS. It was found that Pd-H_2N-PEG had a very short circulation half-life of about 30 min and the maximum blood concentration was ∼25%ID/g (Figure 2a). Biodistribution studies indicated that Pd−H_2N-PEG mainly

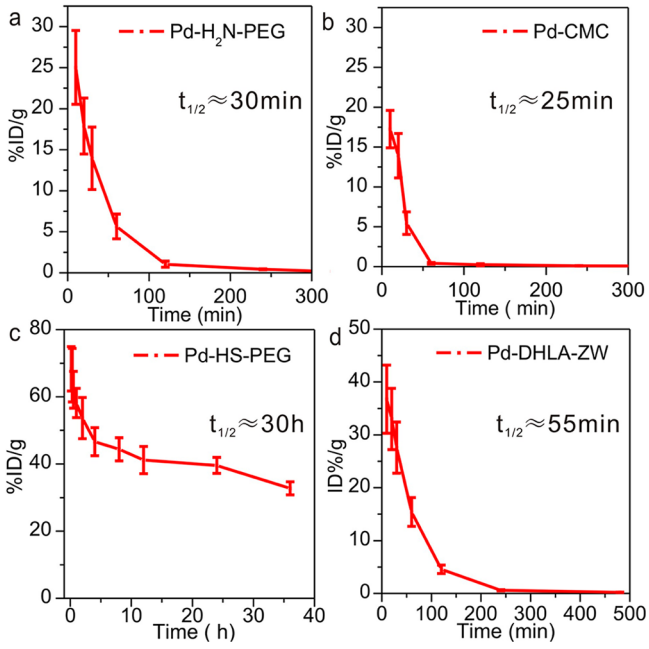

Figure 2. Blood circulation of different ligand modified Pd NSs. (a) Pd-H_2N-PEG, (b) Pd-CMC, (c) Pd-HS-PEG, (d) Pd-DHLA-ZW.

accumulated in the reticuloendothelial system (RES) organs such as liver and spleen (over 40%ID/g in liver and 25% ID/g in spleen). The accumulation amounts in both organs did not reduce with time within 28 days (Figure 3a). Because of the

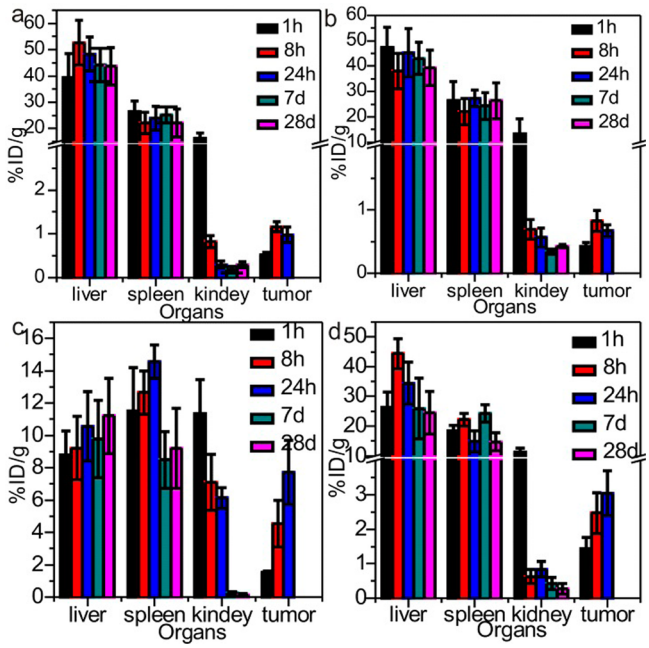

Figure 3. Biodistribution of different ligand modified Pd NSs. (a) Pd-H_2N-PEG, (b) Pd-CMC, (c) Pd-HS-PEG, (d) Pd-DHLA-ZW.

poor blood circulation time of Pd-H_2N-PEG, there was only ∼1% ID/g Pd accumulated in tumor (Figure 3a). The accumulation in kidney was reduced with time, suggesting the possible clearance of Pd-H_2N-PEG through urine.

Considering that there is only one amine group on each polymer chain of PEG, the short blood circulation time of Pd-H_2N-PEG was likely due to the poor binding strength between

DOI: 10.1021/acsami.5b03106
ACS Appl. Mater. Interfaces 2015, 7, 14369−14375

PEG-NH_2 and Pd NSs. Multiple amine groups of surface ligands may improve the stability of ligands on Pd NSs, avoiding the ligands falling away from the surface of the nanoparticles and thus extending the blood circulation time. Following this idea, we further chose CMC, a water-solute sugar with multiple amine groups produced by deacetylation of the abundant biopolymer chitin, to modify Pd NSs.[28] However, it is to our surprise that the blood circulation half-life (~25 min, Figure 2b) and organ distribution (Figure 3b) of the CMC-modified Pd NSs (Pd-CMC) were quite similar to that of Pd-H_2N-PEG. These results suggested that ligands with amine groups might not be good candidates for the surface modification of Pd NSs to inhibit the nonspecific adsorption of biomolecules in blood and thus achieve long blood circulation time.

Considering that thiol groups have strong coordination interaction with noble metals, we further applied ligands containing thiol groups, PEG-SH (5 kDa) and dihydrolipoic acid-zwitterion (DHLA-ZW), for the surface modification of Pd NSs. Indeed, changing from amine to thiol made a significant difference in biobehaviors of Pd NSs. As shown in Figure 2c, the circulation half-life for the Pd NSs modified with PEG-SH (Pd-HS-PEG) reached about 30 h and the maximum blood concentration was up to 70%ID/g (Figure 2c). Because of the prolonged circulation time, the accumulation of Pd-HS-PEG were less than 12%ID/g in liver and 15%ID/g in spleen within 28 days, respectively. The accumulation in tumor increased with time and reached ~8%ID/g at 24 h (Figure 3c). Comparing these results with those of Pd−H_2N-PEG, both of them with the same length of PEG chains, the difference in blood circulation and biodistribution may be due to the different binding strength of thiol groups and amino groups to Pd NSs. That is to say, the binding of amino groups on Pd NSs is not strongly enough to compete the nonspecific adsorption of biomolecules during blood circulation. Once Pd NSs lost this "corona", they were easily swallowed and eliminated by the RES organs.

To confirm the different binding strength of thiol- and amino-bearing ligands to Pd NSs, we used gel filtration chromatography (GFC) to monitor the falling-off of surface ligands from Pd NSs as well as the hydrodynamic diameters (HDs) of the modified Pd NSs (i.e, Pd-HS-PEG, Pd-H_2N-PEG) in biological media. This technique allows online and full spectrum analysis with high reliability and repeatability. In GFC, the retention times of nanoparticles are closely related to their hydrodynamic diameters.[29,30] We first used a group of proteins with different sizes as markers to calibrate the HDs,[30] Blue dextran (M1, 19.0 min, 29.5 nm HD), thyroglobulin (M2, 31.8 min, 18.8 nm HD), alcohol dehydrogenase (M3, 41.7 min, 10.1 nm HD), ovalbumin (M4, 44.8 min, 6.1 nm HD), and vitamin B12 (M5, 55.6 min, 1.5 nm HD) (Figure S2 in the Supporting Information) were chosen. Under the same conditions, the retention times of Pd-HS-PEG and Pd-H_2N-PEG were measured. According to the calibration curve of retention time to HD (Figure S2b in the Supporting Information), the HDs of Pd-HS-PEG and Pd-H_2N-PEG samples were estimated to be about 22 and 21 nm, respectively (Figure 4). In the GFC of Pd-H_2N-PEG, two extra peaks at the retention times of 44 and 53 min, respectively, were observed. These two extra peaks were consistent with free PEG-NH_2 (Figure 4), indicating that PEG-NH_2 did fall off Pd-H_2N-PEG during the blood circulation. Therefore, compared with amine groups, thiol groups can provide stronger coordination interaction with Pd NSs.

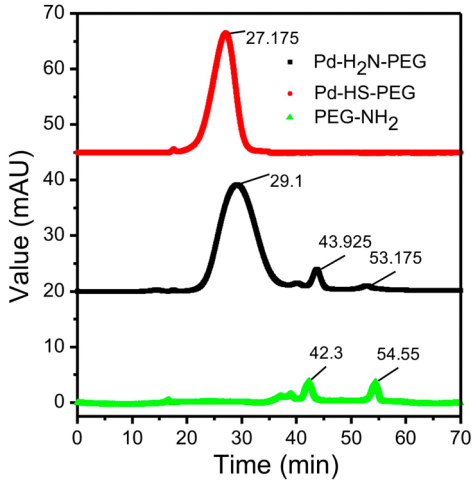

Figure 4. Gel-filtration chromatography (GFC) profiles and size analysis of Pd-HS-PEG and Pd-H_2N-PEG in PBS.

Zwitterionic ligands such as DHLA-ZW which contains two thiol groups, a quaternary ammonium group as well as a sulfonate group, has been reported in the literature to have good water dispersibility and biocompatibility.[31] We expected that the two thiol groups in DHLA-ZW would provide strong coordination with Pd NSs and the zwitterionic character would help to decrease nonspecific interaction with proteins. These two important features would avoid nanoparticles to be rapidly cleared out of the blood. However, to our surprise, as shown in Figure 2d, the half-life and the maximum blood concentration for DHLA-modified Pd NSs (Pd-DHLA-ZW) was only ~55 min and 37%ID/g, respectively. The numbers were far lower than those of Pd-HS-PEG. Consequently, the corresponding Pd amounts in some RES organs (e.g., liver, spleen) were also higher than Pd-HS-PEG (Figure 3c, d). These results suggested that the effect of zwitterionic character of DHLA-ZW in preventing the nonspecific adsorption of protein was not as good as PEG-SH. PEG-SH might be the best choice to modify Pd NSs for the in vivo applications in cancer therapy.

3.3. Potential Toxicity of Different Surface-Coated Pd NSs. To determine both in vitro and in vivo biocompatibility of Pd NSs coated by different organic ligands, we carried out standard MTT assay, blood biochemistry, and histological analyses. As shown in Figure S3 in the Supporting Information, the MTT results indicated that various modified Pd NSs had very good biocompatibility, and the viability of HeLa cells still kept above 85% when incubated with different Pd NSs in the concentration range up to 150 μg/mL for 24 h (Figure S3, Supporting Information).

Because high accumulation of nanoparticles in liver may lead to damage to this tissue, a serum biochemistry assay was also performed to evaluate the potential toxic effect of these modified Pd NSs in liver. Two biochemical parameters such as alanine aminotransferase (ALT) and aspartate aminotransferase (AST) were tested. Blood from mice injected with various modified Pd NSs and age-matched untreated mice was collected at 7 days post injection. As shown in Figure 5a, compared with the control group, no obvious hepatic toxicity was observed after intravenous injection of various modified Pd NSs for 7 days. In addition, H&E stained images of major organs including spleen, kidney, liver, heart, and lung were

DOI: 10.1021/acsami.5b03106
ACS Appl. Mater. Interfaces 2015, 7, 14369−14375

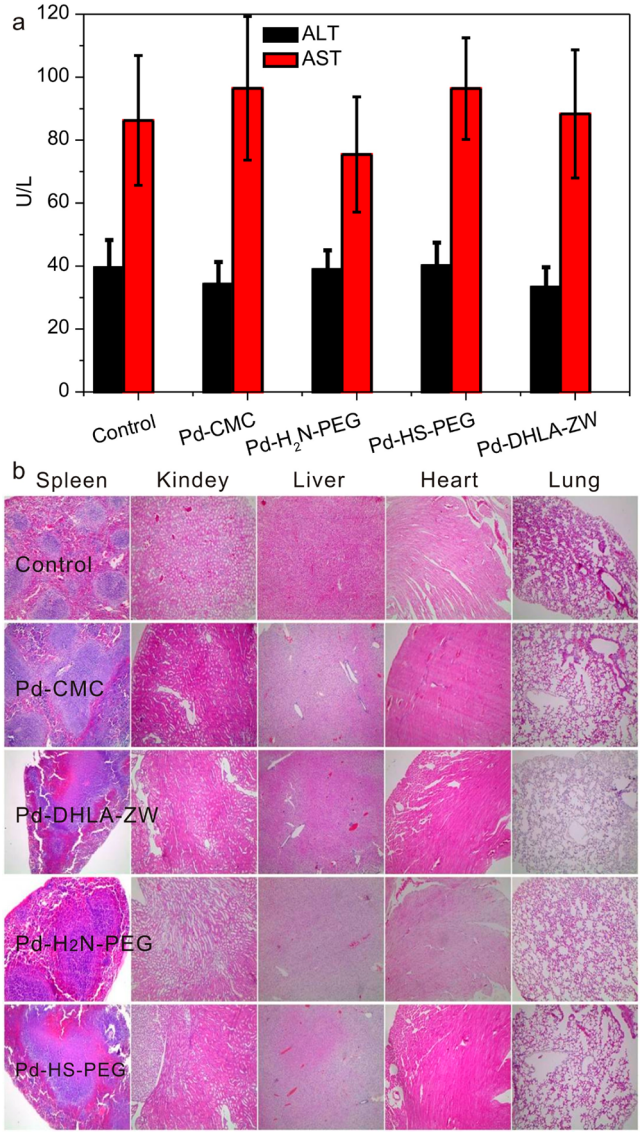

Figure 5. (a) Serum biochemistry analysis of mice treated with different coated Pd NSs at 7 days post injection. (b) Photos of H&E stained diaphragm slices from the mice treated with different coated Pd NSs at 28 days post injection.

collected from the untreated mice and injected mice at 28 days and no detectable organ damages were observed either (Figure 5b). These results collectively demonstrate that different organic coated Pd NSs possess no noticeable toxic to mice in vivo. However, more effort is still required to systematically examine the potential long-term toxicity of modified Pd NSs at various doses in animals.

3.4. Optimum Coating Amount and Molecular Weight of PEG-SH and the Renal Clearance of Pd-HS-PEG with Time. It was reported that the amount of coating molecules would affect the blood circulation half-life and tissue distribution of nanomaterials.[32] Because PEG-SH has been proved to be the best ligand to coat Pd NSs among the studied coating molecules, we further investigated the effects of PEG-SH adding amounts on the circulation time of Pd NSs. As illustrated in Figure 6a, as the mass ratio of PEG-SH to Pd NSs increased from 1:4 to 4:1, the circulation half-lives of Pd-HS-PEG increased from 20 to 32 h (Figure 6a). The results indicated that even with small amount of PEG-SH, Pd NSs still

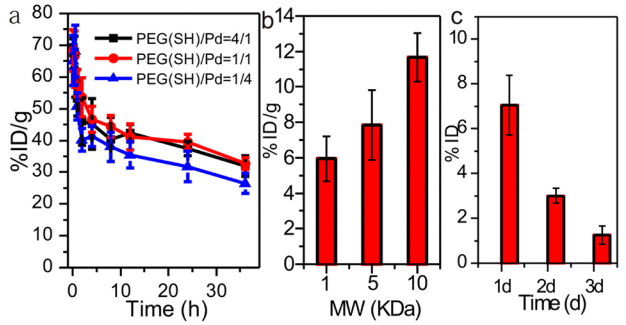

Figure 6. (a) Blood circulation of different amount PEG-SH-modified Pd nanosheets. (b) Tumor accumulation of Pd-HS-PEG with different PEG-SH molecular weight. (c) In vivo clearance of Pd-HS-PEG within 3 days.

kept long circulation time in vivo, further confirming the strong interaction of PEG-SH with Pd NSs. Therefore, we chose the Pd-HS-PEG with the 1:1 mass ratio of PEG-SH to Pd NSs ($t_{1/2}$ ≈ 30 h) for the therapeutic experiments. Besides, the effects of PEG-SH with different molecular weights on the tumor uptake of Pd NSs were also investigated. As shown in Figure 6b, the PEG-SH (1 kDa)-modified Pd NSs showed the lowest tumor uptake about 6%ID/g, whereas PEG-SH (10 kDa) modified Pd NSs have the highest tumor uptake ~12%ID/g. The results indicated that through choosing appropriate coating molecular weights, the nanoparticle uptake efficiency by tumor can be further increased.

Generally, the potential toxicity of nanoparticles and the chance for them to interfere with the function of different tissues can be minimized if they are cleared from the body within a reasonable period.[33] As observed from the biodistribution data in Figure 3, different surface-modified Pd NSs could accumulate in kidney and decrease with time, indicating the potential of renal clearance of Pd NSs. Here, we further quantity the amount of renal excretion of Pd-HS-PEG. Dose of 200 μg of Pd-HS-PEG was intravenously administered. Urine was collected within a 3-day period after administration. ICP-MS was used to measure the Pd concentration in the urine at different time points post injection. As shown in Figure 6c, 11.5% of Pd-HS-PEG were cleared through renal into urine within 3 days, and most happened on the first day (about 61% of the total amount, 27.8% on the second day and 11.2% on the third day. The long circulation time of Pd-HS-PEG in bloodstream is expected to provide them more chance to contact with kidney and go through the renal filtration to be cleared. The surface modification of PEG-SH not only improves the in vivo blood circulation of Pd NSs, making them easily accumulated at target organs, but also makes nanoparticles to be better cleared through urine.

3.5. In Vivo Anticancer Effects of Pd-HS-PEG. The excellent accumulation performance in tumor of Pd-HS-PEG encouraged us to pursue their application as an effective photothermal agent in in vivo photothermal therapy. When the tumor volume grew to approximately 70 mm^3, the mice bearing S180 tumor were randomly separated into two groups (five mice per group) and each mice was intravenously injected with 300 μL of PBS or 300 μL of a PBS dispersion of Pd-HS-PEG (1 mg/mL). After injection, the tumors were then exposed to an 808 nm laser with a power density of 0.4 W/cm^2 for 5 min. During the laser irradiation, full-body thermographic images were recorded by an infrared camera (Figure 7a). For the Pd-

DOI: 10.1021/acsami.5b03106
ACS Appl. Mater. Interfaces 2015, 7, 14369−14375

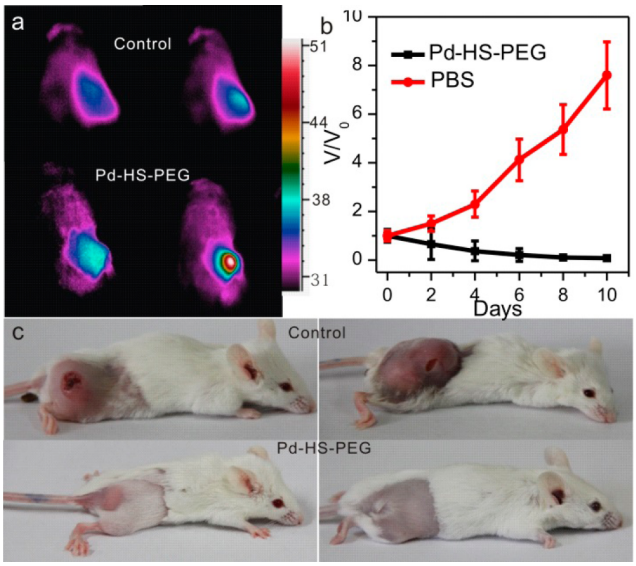

Figure 7. (a) Infrared thermal images of tumor-bearing mice with PBS and Pd-HS-PEG injection under 0.4 W/cm^2 808 nm laser irradiation. (b) Relative tumor volume of different groups. (c) Photographs of the Pd-HS-PEG nanoparticles and PBS-treated mice taken before and 9 days after laser irradiation.

HS-PEG treated mice, the tumor temperature increased quickly from 35 to 52 °C after 5 min of laser exposure, which was high enough to ablate tumors. In comparison, only a 3 °C temperature increase was observed for the saline injected mice. As shown in Figure 7b, the tumor volume for the control group which were treated with PBS and irradiated by the 808 nm laser increased with time (red line in Figure 7b). In sharp contrast, the tumor growth was remarkably suppressed in the Pd-HS-PEG treated group (black line in Figure 7b). All irradiated tumors on mice injected with Pd-HS-PEG disappeared after 9 days and no tumor regrowth was observed in this treated group. In comparison, rapid tumor growth was observed in the PBS treated control group (Figure 7c). These results clearly revealed that the Pd-HS-PEG nanoparticles have the ability to induce hyperthermia by converting the 808 nm NIR light energy to heat in vivo and thus enable the effective photothermal ablation of tumors.

4. CONCLUSION

In summary, we have systematically investigated the effects of different surface coatings on the blood circulation, biodistribution and potential toxicity of Pd NSs. Among the four different coatings, PEG-NH_2, CMC, PEG-SH, and DHLA-ZW, PEG-SH-modified Pd NSs (Pd-HS-PEG) showed the longest circulation half-life and the highest tumor accumulation. All these functionalized Pd NSs exhibited no obvious hepatic toxicity by blood biochemistry assay and no detectable organ damage by H&E stained imaging. Gel filtration chromatography (GFC) experiments revealed that with the similar PEG chain length and hydrodynamic diameters (HDs), PEG-SH-coated Pd NSs displayed better stability than PEG-NH_2-coated counterparts. By optimizing amount of PEG-SH on Pd NSs, the tumors were effectively ablated under the irradiation of 808 nm laser (0.4 W/cm^2) after intravenous administration of Pd-HS-PEG. Our study indicates that the careful design of surface chemistry is important to modulate the bioproperties of Pd NSs, providing a guideline for the development of other surface-modified nanoparticles in biomedical applications.

■ ASSOCIATED CONTENT

Supporting Information

Further details of the absorption spectra of different surface-coated Pd NSs dispersed in PBS for 1 and 8 h, zeta potentials of different surface-coated Pd NSs, retention times of protein with different sizes as markers, calibration curve of the retention time to the diameter, viability of HeLa cells incubated with surface-coated Pd NSs with different concentrations for 24 h, and blood circulation times of different amounts of PEG-SH-modified Pd nanosheets. The Supporting Information is available free of charge on the ACS Publications website at DOI: 10.1021/acsami.5b03106.

■ AUTHOR INFORMATION

Corresponding Authors

*E-mail: chenxl@xmu.edu.cn.
*E-mail: nfzheng@xmu.edu.cn.

Notes

The authors declare no competing financial interest.

■ ACKNOWLEDGMENTS

The work was supported by the National Natural Science Foundation of China (21101131), National Basic Research Foundation (973) of China (2014CB932004), Natural Science Foundation of Fujian Province (No.2012J01056), Fundamental Research Funds for the Central Universities (2010121015), and the open project grant from State Key Laboratory of Chemo/biosensing and Chemometrics (2013009).

■ REFERENCES

(1) Ferrari, M. Cancer Nanotechnology: Opportunities and Challenges. *Nat. Rev. Cancer* **2005**, *5*, 161−171.
(2) Cai, W.; Chen, X. Nanoplatforms for Targeted Molecular Imaging in Living Subjects. *Small* **2007**, *3*, 1840−1854.
(3) Peer, D.; Karp, J. M.; Hong, S.; FarokHzad, O. C.; Margalit, R.; Langer, R. Nanocarriers as an Emerging Platform for Cancer Therapy. *Nat. Nanotechnol.* **2007**, *2*, 751−760.
(4) Yang, K.; Wan, J.; Zhang, S.; Zhang, Y.; Lee, S.-T.; Liu, Z. In Vivo Pharmacokinetics, Long-Term Biodistribution, and Toxicology of PEGylated Graphene in Mice. *ACS Nano* **2010**, *5*, 516−522.
(5) Cheng, L.; Yang, K.; Shao, M.; Lu, X.; Liu, Z. In Vivo Pharmacokinetics, Long-Term Biodistribution and Toxicology Study of Functionalized Upconversion Nanoparticles in Mice. *Nanomedicine* **2011**, *6*, 1327−1340.
(6) Aillon, K. L.; Xie, Y.; El-Gendy, N.; Berkland, C. J.; Forrest, M. L. Effects of Nanomaterial Physicochemical Properties on in Vivo Toxicity. *Adv. Drug Delivery Rev.* **2009**, *61*, 457−466.
(7) Soo Choi, H.; Liu, W.; Misra, P.; Tanaka, E.; Zimmer, J. P.; Itty Ipe, B.; Bawendi, M. G.; Frangioni, J. V. Renal Clearance of Quantum Dots. *Nat. Biotechnol.* **2007**, *25*, 1165−1170.
(8) Doshi, N.; Mitragotri, S. Designer Biomaterials for Nanomedicine. *Adv. Funct. Mater.* **2009**, *19*, 3843−3854.
(9) Mitragotri, S.; Lahann, J. Physical Approaches to Biomaterial Design. *Nat. Mater.* **2009**, *8*, 15−23.
(10) Stewart, M. H.; Susumu, K.; Mei, B. C.; Medintz, I. L.; Delehanty, J. B.; Blanco-Canosa, J. B.; Dawson, P. E.; Mattoussi, H. Multidentate Poly(ethylene glycol) Ligands Provide Colloidal Stability to Semiconductor and Metallic Nanocrystals in Extreme Conditions. *J. Am. Chem. Soc.* **2010**, *132*, 9804−9813.
(11) Susumu, K.; Uyeda, H. T.; Medintz, I. L.; Pons, T.; Delehanty, J. B.; Mattoussi, H. Enhancing the Stability and Biological Functionalities

DOI: 10.1021/acsami.5b03106
ACS Appl. Mater. Interfaces 2015, 7, 14369−14375

of Quantum Dots via Compact Multifunctional Ligands. *J. Am. Chem. Soc.* **2007**, *129*, 13987−13996.
(12) Liu, S. J.; Han, Y. C.; Qiao, R. R.; Zeng, J. F.; Jia, Q. J.; Wang, Y. L.; Gao, M. Y. Investigations on the Interactions between Plasma Proteins and Magnetic Iron Oxide Nanoparticles with Different Surface Modifications. *J. Phys. Chem. C* **2010**, *114*, 21270−21276.
(13) Cedervall, T.; Lynch, I.; Lindman, S.; Berggard, T.; Thulin, E.; Nilsson, H.; Dawson, K. A.; Linse, S. Understanding the Nanoparticle-Protein Corona Using Methods to Quantify Exchange Rates and Affinities of Proteins for Nanoparticles. *Proc. Natl. Acad. Sci. U.S.A.* **2007**, *104*, 2050−2055.
(14) Sahoo, B.; Goswami, M.; Nag, S.; Maiti, S. Spontaneous Formation of a Protein Corona Prevents the Loss of Quantum Dot Fluorescence in Physiological Buffers. *Chem. Phys. Lett.* **2007**, *445*, 217−220.
(15) Lynch, I.; Dawson, K. A. Protein-Nanoparticle Interactions. *Nano Today* **2008**, *3*, 40−47.
(16) Simpson, C. A.; Agrawal, A. C.; Balinski, A.; Harkness, K. M.; Cliffel, D. E. Short-Chain PEG Mixed Monolayer Protected Gold Clusters Increase Clearance and Red Blood Cell Counts. *ACS Nano* **2011**, *5*, 3577−3584.
(17) Gref, R.; Domb, A.; Quellec, P.; Blunk, T.; Müller, R. H.; Verbavatz, J. M.; Langer, R. The Controlled Intravenous Delivery of Drugs Using PEG-Coated Sterically Stabilized Nanospheres. *Adv. Drug Delivery Rev.* **1995**, *16*, 215−233.
(18) Passirani, C.; Barratt, G.; Devissaguet, J. P.; Labarre, D. Long-Circulating Nanoparticles Bearing Heparin or Dextran Covalently Bound to Poly(methyl methacrylate). *Pharm. Res.* **1998**, *15*, 1046−1050.
(19) Xiao, W.; Lin, J.; Li, M.; Ma, Y.; Chen, Y.; Zhang, C.; Li, D.; Gu, H. Prolonged in Vivo Circulation Time by Zwitterionic Modification of Magnetite Nanoparticles for Blood Pool Contrast Agents. *Contrast Media Mol. Imaging* **2012**, *7*, 320−327.
(20) Chen, M.; Tang, S.; Guo, Z.; Wang, X.; Mo, S.; Huang, X.; Liu, G.; Zheng, N. Core-Shell Pd@Au Nanoplates as Theranostic Agents for In-Vivo Photoacoustic Imaging, CT Imaging, and Photothermal Therapy. *Adv. Mater.* **2014**, *26*, 8210−8216.
(21) Zhao, Z.; Shi, S.; Huang, Y.; Tang, S.; Chen, X. Simultaneous Photodynamic and Photothermal Therapy Using Photosensitizer-Functionalized Pd Nanosheets by Single Continuous Wave Laser. *ACS Appl. Mater. Interfaces* **2014**, *6*, 8878−8885.
(22) Huang, X.; Tang, S.; Mu, X.; Dai, Y.; Chen, G.; Zhou, Z.; Ruan, F.; Yang, Z.; Zheng, N. Freestanding Palladium Nanosheets with Plasmonic and Catalytic Properties. *Nat. Nanotechnol.* **2011**, *6*, 28−32.
(23) Tang, S. H.; Chen, M.; Zheng, N. F. Sub-10-nm Pd Nanosheets with Renal Clearance for Efficient Near-Infrared Photothermal Cancer Therapy. *Small* **2014**, *10*, 3139−3144.
(24) Zhao, Z. X.; Huang, Y. Z.; Shi, S. G.; Tang, S. H.; Li, D. H.; Chen, X. L. Cancer Therapy Improvement with Mesoporous Silica Nanoparticles Combining Photodynamic and Photothermal Therapy. *Nanotechnology* **2014**, *25*, 285701.
(25) Owens, D. E., III; Peppas, N. A. Opsonization, Biodistribution, and Pharmacokinetics of Polymeric Nanoparticles. *Int. J. Pharm.* **2006**, *307*, 93−102.
(26) Liu, J.; Yu, M.; Ning, X.; Zhou, C.; Yang, S.; Zheng, J. PEGylation and Zwitterionization: Pros and Cons in the Renal Clearance and Tumor Targeting of Near-IR-Emitting Gold Nanoparticles. *Angew. Chem., Int. Ed.* **2013**, *52*, 12804−12808.
(27) Knop, K.; Hoogenboom, R.; Fischer, D.; Schubert, U. S. Poly(ethylene glycol) in Drug Delivery: Pros and Cons as Well as Potential Alternatives. *Angew. Chem., Int. Ed.* **2010**, *49*, 6288−6308.
(28) Makhubela, B. C.; Jardine, A.; Smith, G. S. Pd Nanosized Particles Supported on Chitosan and 6-Deoxy-6-Amino Chitosan as Recyclable Catalysts for Suzuki−Miyaura and Heck Cross-Coupling Reactions. *Appl. Catal., A* **2011**, *393*, 231−241.
(29) Liu, F. K. Using SEC for Analyzing the Sizes of Au/Pt Core/Shell Nanoparticles. *Chromatographia* **2010**, *72*, 473−480.
(30) Zhou, Z.; Wang, L.; Chi, X.; Bao, J.; Yang, L.; Zhao, W.; Chen, Z.; Wang, X.; Chen, X.; Gao, J. Engineered Iron-Oxide-Based Nanoparticles as Enhanced T1 Contrast Agents for Efficient Tumor Imaging. *ACS Nano* **2013**, *7*, 3287−3296.
(31) Kim, D.; Chae, M. K.; Joo, H. J.; Jeong, I.-h.; Cho, J.-H.; Lee, C. Facile Preparation of Zwitterion-Stabilized Superparamagnetic Iron Oxide Nanoparticles (ZSPIONs) as an MR Contrast Agent for in Vivo Applications. *Langmuir* **2012**, *28*, 9634−9639.
(32) Liu, X.; Tao, H.; Yang, K.; Zhang, S.; Lee, S.-T.; Liu, Z. Optimization of Surface Chemistry on Single-Walled Carbon Nanotubes for in Vivo Photothermal Ablation of Tumors. *Biomaterials* **2011**, *32*, 144−151.

DOI: 10.1021/acsami.5b03106
ACS Appl. Mater. Interfaces 2015, 7, 14369−14375